# Hydrogen Activation by an Aromatic Triphosphabenzene

Lauren E. Longobardi,[†] Christopher A. Russell,[‡] Michael Green,[‡] Nell S. Townsend,[‡] Kun Wang,[⊥] Arthur J. Holmes,[∥] Simon B. Duckett,[∥] John E. McGrady,[§] and Douglas W. Stephan*,[†,¶]

[†]Department of Chemistry, University of Toronto, 80 St. George Street, Toronto, Ontario, Canada M5S 3H6
[‡]School of Chemistry, University of Bristol, Cantock's Close, Bristol BS8 1TS, United Kingdom
[§]Department of Chemistry, University of Oxford, South Parks Road, Oxford OX1 3QR, United Kingdom
[∥]Department of Chemistry, University of York, York, YO10 5DD, United Kingdom
[⊥]State Key Laboratory of Explosion Science and Technology, Beijing Institute of Technology, Beijing 100081, P. R. China
[¶]Chemistry Department, Faculty of Science, King Abdulaziz University (KAU), Jeddah 21589, Saudi Arabia

S *Supporting Information*

ABSTRACT: Aromatic hydrogenation is a challenging transformation typically requiring alkali or transition metal reagents and/or harsh conditions to facilitate the process. In sharp contrast, the aromatic heterocycle 2,4,6-tri-*tert*-butyl-1,3,5-triphosphabenzene is shown to be reduced under 4 atm of H_2 to give [3.1.0]bicylo reduction products, with the structure of the major isomer being confirmed by X-ray crystallography. NMR studies show this reaction proceeds via a reversible 1,4-H_2 addition to generate an intermediate species, which undergoes an irreversible suprafacial hydride shift concurrent with P−P bond formation to give the isolated products. Further, *para*-hydrogen experiments confirmed the addition of H_2 to triphosphabenzene is a bimolecular process. Density functional theory (DFT) calculations show that facile distortion of the planar triphosphabenzene toward a boat-conformation provides a suprafacial combination of vacant acceptor and donor orbitals that permits this direct and uncatalyzed reduction of the aromatic molecule.
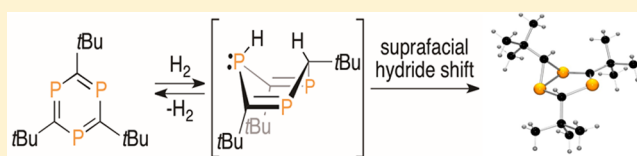
INTRODUCTION

The cleavage of the simplest molecule, dihydrogen (H_2), is the instrumental step to hydrogenation reactions used in a myriad of industrial processes[1−7] and is the key reaction in a number of hydrogenase enzymes[8−10] and related biological systems.[11] It was in the early 20th century that Sabatier[12] uncovered amorphous metals which catalyze hydrogenations, while the emergence and evolution of organometallic chemistry provided homogeneous precious metal catalysts[13−22] and more recently earth-abundant metal systems.[23−25] Non-transition metal compounds including KO*t*Bu[26] and calcium-hydride species[27] have also been reported to catalyze the hydrogenation of selected substrates. Non-metal, main group elements were initially shown to react with H_2 by low temperature matrix[28−30] and computational studies.[31,32] Subsequently, reactions with germynes[33] were described, but more recently, main group systems have been documented as effective metal-free hydrogenation catalysts[34−36] with the advent of frustrated Lewis pairs (FLPs).[37]

Understanding these reactions with H_2 in terms of the orbitals involved uncovers the underlying similarities of transition metal and main group systems.[38] For transition metals, the combination of vacant d-orbitals accepting electron density from the H−H σ-bond and filled d-orbitals donating electron density into the σ*-orbital of H_2 enables H−H bond cleavage (Figure 1a). In the same vein, main group systems[33,37,39−41] shown to activate hydrogen present ground
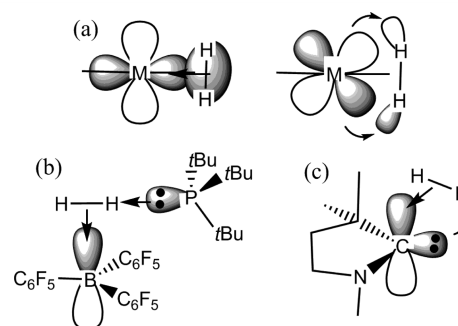

Figure 1. Activation of H_2.

state acceptor and donor orbitals that can interact with H_2 to effect the heterolytic cleavage of the H−H bond (Figure 1b,c). On the basis of this seemingly general criterion, aromatic species would not be expected to activate H_2. Indeed, these notoriously stable molecules[42] lack accessible donor-acceptor orbitals needed to facilitate H_2 cleavage, and thus aromatic hydrogenations require a catalyst to preactivate the H−H bond.[43−47]
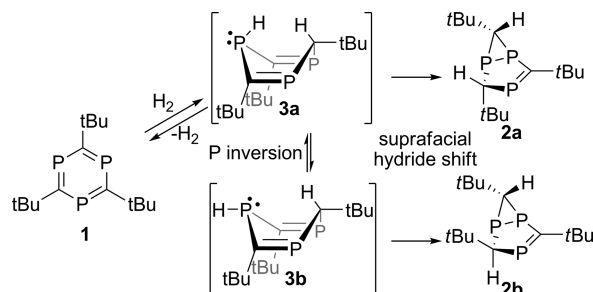
Our recent finding that FLP hydrogenations using $B(C_6F_5)_3$ and sterically encumbered anilines[48] resulted in the corresponding saturated cyclohexylammonium salts prompted us to

explore the corresponding hydrogenation of 2,4,6-tri-*tert*-butyl-1,3,5-triphosphabenzene **1**[49] (Scheme 1). Herein we report that

Scheme 1. Proposed Mechanism for H$_2$ Activation

although the planar[50] phosphorus-based heterocycle triphosphabenzene is aromatic,[51−53] it reacts with H$_2$ in an uncatalyzed process. The nature of the products is established and the unexpected mechanism of formation has been established by *para*-hydrogen experiments and computational studies.

■ RESULTS AND DISCUSSION

The aromatic molecule **1**[51−53] was treated with 5 mol% B(C$_6$F$_5$)$_3$ under 4 atm of H$_2$ at 110 °C for 5 h in C$_6$D$_5$Br and found to react quantitatively to give the isomeric bicyclic compounds **2a** and **2b**.[54,55] Interestingly, control experiments revealed that reaction of **1** alone with 4 atm of H$_2$ at 110 °C in C$_6$D$_5$Br also led to the clean formation of **2a** and **2b**. Indeed, monitoring this uncatalyzed hydrogenation over the course of the reaction resulted in the consumption of **1** and the generation of **2a/2b** at comparable rates in the presence or absence of B(C$_6$F$_5$)$_3$. As compound **1** is prepared by the cyclotrimerization of *t*BuC≡P by Cl$_3$V═N*t*Bu,[56−59] the hydrogenation of **1** was explored in the presence of added Cl$_3$V═N*t*Bu. However, the rate of formation of **2a/2b** was unaffected by this additive. Collectively these data affirm the direct reaction of **1** with H$_2$ affords the products **2a/2b**. Previous literature has reported the independent formation of **2a** and **2b** from reactions of unsaturated P−C bonds at Hf and Ga centers.[54,55]

The isomeric products **2a** and **2b** were isolated by slow concentration resulting in the formation of pale-yellow crystals. ^{31}P NMR data showed the intensity ratio of the resonances attributed to **2a** and **2b**, respectively, was 4:1. In the corresponding ^{1}H NMR spectrum, **2a** exhibited resonances at 2.98, 1.49, 1.13, and 0.92 ppm, while **2b** gave peaks at 2.59, 1.46, 1.28, and 0.93 ppm. Assignment of these resonances and the ^{13}C NMR data were confirmed with ^{31}P-HMBC and HSQC spectra and further supported by the corresponding characterization of **2a−d$_2$/2b−d$_2$**. The major isomer **2a** was further characterized by X-ray crystallography (Figure 2).

The mechanism of this reduction was probed by monitoring the reaction by ^{31}P NMR spectroscopy at room temperature. After 24 h, about 14% of **1** is converted to a species **3** (Scheme 1). Upon heating to 110 °C, both **1** and **3** were consumed, affording **2a/2b** as the final products in 5 h. The ^{31}P NMR spectrum of this intermediate **3** shows resonances at 240 and −24.8 ppm ([1]J_{PH} = 229 Hz) in a 2:1 ratio. This break in P atom symmetry taken with the large one-bond P−H coupling constant is consistent with the formulation of **3** as the product of 1,4-addition of H$_2$ to **1**. This intermediate has been previously observed as one of the products of hydrolysis of Hf
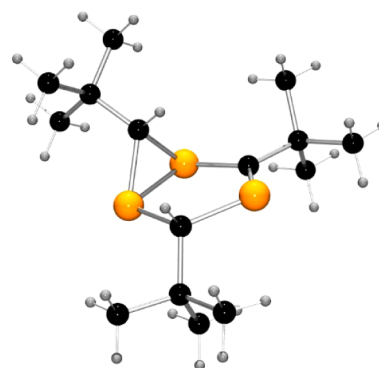

Figure 2. POV-ray depiction of the molecular structure of **2a**; color scheme: P, orange; C, black; H, gray. Selected bond distances and angles: five membered ring, C═P, 1.689(3) Å; C−P, 1.850(4) Å, 1.871(3) Å, 1.832(3) Å; P−P, 2.196(1) Å; three membered ring, C−P, 1.830(4) Å, 1.865(4) Å; C−P−P, 54.3(1)°, 52.8(1)°; P−C−P, 72.9(1)°.

complexes of P−C multiple bonds.[54] The subsequent migration of the PH hydride to the adjacent carbon with concurrent P−P bond formation to give **2a/2b** is thermally driven (Scheme 1). The existence of conformational isomers of 1,3,5-triphosphacyclohexa-1,4-dienes **3** provides an explanation for the observation of two isomers, **2a** and **2b**, as the final products.

This reaction of **1** was also explored with *para*-hydrogen (*p*-H$_2$),[60] a technique which has been used very successfully to study metal catalyzed reactions.[61] When a sample of **1** was warmed to 110 °C in C$_6$D$_5$Br in the presence of *p*-H$_2$, two polarized proton signals appear due to compound **3** at 6.4 and 1.8 ppm (Figure 3). Importantly, the spin-encoding associated with *p*-H$_2$ is retained, which supports the suggested intramolecular activation mechanism, and interestingly, a substantial signal gain is evident for a period of many minutes, indicative of the reversible formation of **3** from **1**. The signal at 6.4 ppm exhibits a strong PH coupling of 227 Hz, and two smaller P−P splittings of 6.5 Hz in addition to the antiphase proton splitting of +1.5 Hz to the resonance at 1.95 ppm. A 2D [1]H−[31]P HMQC located the ^{31}P signals for this species at 237.2 and −30.6 with the selective decoupling experiments confirming that the PH signal arises from the high field resonance. The observation of *p*-H$_2$ addition to a nonmetal system is unusual, with the Koptyug's observation of H$_2$ addition to an amino borane providing the only other metal-free example.[62] When used in conjunction with the OPSY(only *para*-hydrogen spectroscopy) protocol, a strong signal is still retained, thereby confirming the pairwise nature of this process.[63]

Further insights into this aromatic hydrogen activation chemistry come from a survey of the computed potential energy surface for the reaction of H$_2$ with the simplified model (PCMe)$_3$ **1′** (primes denotes the computational models with Me substituents in place of *t*Bu). A free energy surface was computed using gradient-corrected density functional theory[64] with empirical dispersion corrections (BP86-GD3BJ/6-311++G(3d,2p) (Figure 4).[65−67] Parallel calculations performed using Møller−Plesset perturbation theory[68] (MP2/cc-pVTZ) are summarized in the Supporting Information (Figure S10): there are no significant differences between the two model chemistries. The optimized structure of the model reactant **1′** is very similar to the previously reported crystallographic data for **1**, with three equivalent C═P bond lengths of 1.75 Å (cf. 1.727 Å from X-ray[50]) and a planar C$_3$P$_3$ core. The key hydrogen
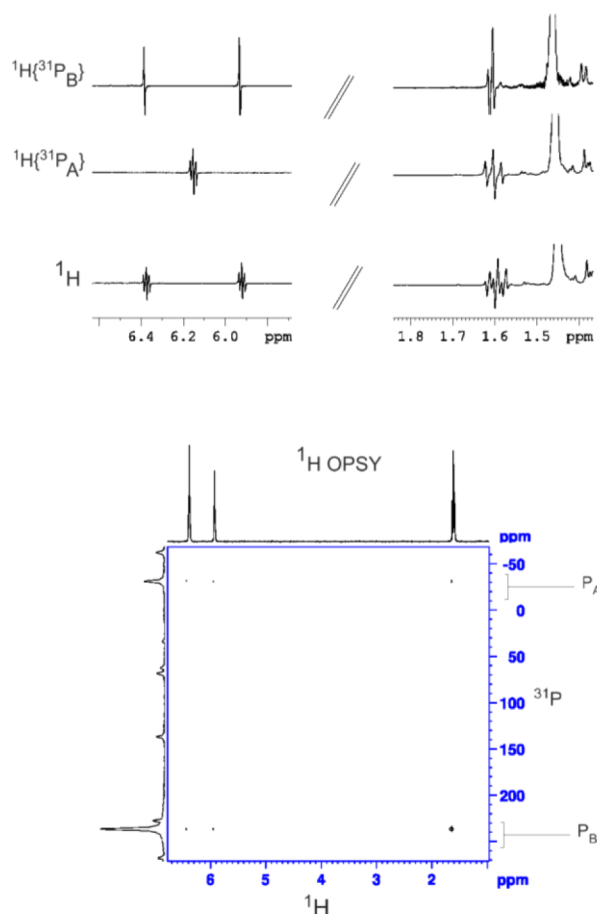
Figure 3. p-H$_2$ 1D and 2D NMR data.

activation step occurs via a 1,4 addition wherein the H$_2$ approaches from above the plane with the H–H vector aligned parallel to the 1–4 axis of the ring. The computed free energy barrier of 28 kcal/mol for this step (at 298 K) is consistent with the elevated temperatures and high pressures needed to accelerate the reaction: it is somewhat larger than those reported by Frenking *et al.*[69] for the reaction of digermynes with H$_2$ which proceed at room temperatures and ambient pressures.

At the transition state **TS1′**, the H–H bond is only marginally elongated from its equilibrium value (0.85 vs 0.75 Å in H$_2$), but nevertheless, the P and C centers are distorted significantly out of the plane such that the C$_3$P$_3$ unit adopts a boat conformation.[70] In the absence of H$_2$, the boat distortion of the triphosphabenzene ring corresponds to a very low-frequency mode (92 cm^{-1}), suggesting that the innate flexibility of the ring is an important factor in facilitating the activation process. The distortion of **1** to a boat conformation has been previously observed experimentally in a cationic Au(PR$_3$) complex of **1**.[52] NICS-1 calculations revealed that a high degree of aromaticity is maintained in this structural arrangement, in contrast to corresponding carbocyclic ring systems which become antiaromatic with the same deformation. A natural population analysis of **1′** reveals a substantial polarization of the C–P bonds (q(C) = −0.78, q(P) = +0.74); moreover, the negative charge on C1 increases at **TS1′** (−0.85 vs −0.80 for the other two carbons in the ring), suggesting that the deformation of **1′** to a boat conformation enhances its zwitterionic character. An NBO analysis of the interactions between the H$_2$ and C$_3$P$_3$ units at the transition state (**TS1′**) confirms that the dominant interactions are donation of electron density (i) from a C–P π orbital localized on C to H–H σ* and (ii) from H–H σ to a C–P π* orbital localized
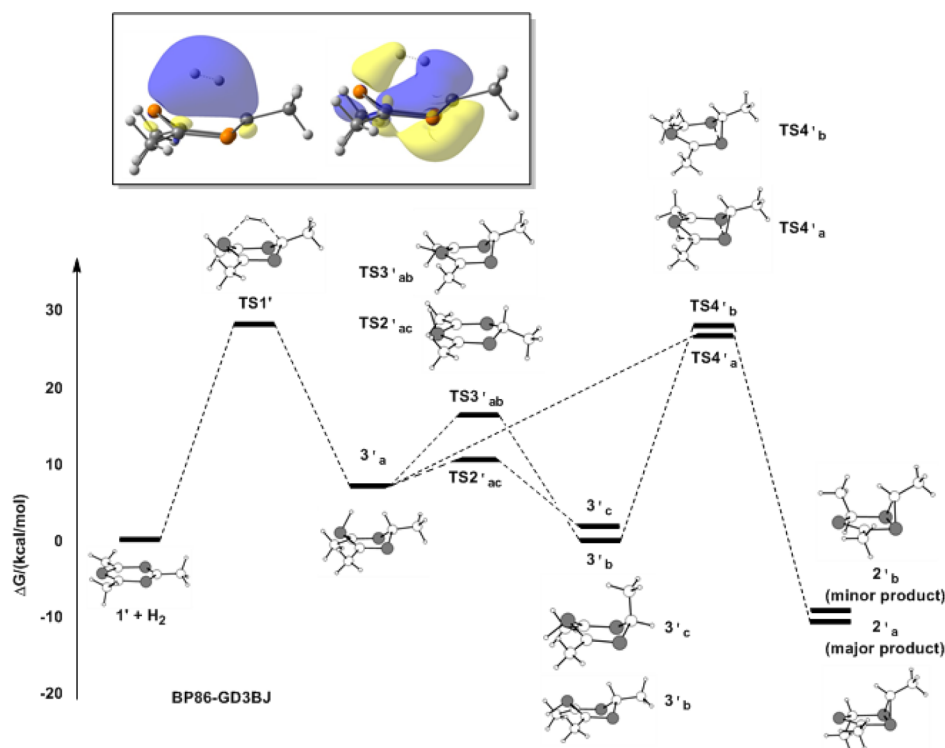

Figure 4. Reaction coordinate for the hydrogenation of **1′** (free energies at 298 K computed at the BP86-GD3BJ level of theory). NLMOs of the transition state **TS1′** are boxed. (NB **3′$_d$** is not shown).

on P (Figure 4 and Supporting Information, Figure S11). The overall picture of the activation process is therefore similar to that discussed in other main-group systems, with acceptor/donor interactions between the σ and σ^* orbitals of H_2 and the polarized frontier orbitals of the substrate.

Transition state $\mathbf{TS1'}$ connects the reactant to intermediate $\mathbf{3'_a}$ (Figure 2) which lies 7 kcal/mol above the reactants. In $\mathbf{3'_a}$ the 1,3,5-triphosphacyclohexa-1,4-diene adopts the boat conformation typical of the 1,4 cyclohexadienes, with the two hydrogens that originate from H_2 in apical positions. $\mathbf{3'_a}$ is not, however, the most stable conformation of the system, and in fact three further structures, $\mathbf{3'_{b-d}}$, were located which differ from $\mathbf{3'_a}$ in the configuration at phosphorus and/or at the sp^3 hybridized carbon. Of these, $\mathbf{3'_b}$ and $\mathbf{3'_c}$, where the hydrogen on phosphorus is equatorial, are the most stable, lying 6–7 kcal/mol below $\mathbf{3'_a}$ and therefore isoenergetic with the reactants. Interconversion of the various isomers of $\mathbf{3'}$, either via inversion at the phosphorus center ($\mathbf{TS3'_{ab}}$, DG‡ 15 kcal/mol) or via a planar transition state that connects two boat structures ($\mathbf{TS2'_{ac}}$, DG‡ 10 kcal/mol), is more facile than the subsequent hydrogen migration step (vide infra). Intermediate **3** should therefore reach an equilibrium distribution of conformations dominated by $\mathbf{3_b}$ and $\mathbf{3_c}$ prior to rearrangement to the product. To verify this structural assignment, we have computed ^{31}P chemical shifts for the isomers at the BP86-GD3BJ level (see Supporting Information, Figure S12 and Table S1). The computed values for $\mathbf{3'_b}$ and $\mathbf{3'_c}$ are much more consistent with the spectroscopic data detected for **3** than those for $\mathbf{3'_a}$ or $\mathbf{3'_d}$.

The most stable isomer of $\mathbf{3'}$ ($\mathbf{3'_b}$) is connected to the minor product, $\mathbf{2'_b}$, via $\mathbf{TS4'_b}$ with a barrier of 28 kcal/mol. The transition structure is typical of a suprafacial hydride migration, with the migrating hydrogen located between the C and P atoms in an almost perfectly planar C_2P_3 unit. The incipient P–P bond is partially formed at the transition states (P–P 2.90 vs 3.20 Å in $\mathbf{3'_b}$ and 2.25 Å in $\mathbf{2'_b}$). The major product, $\mathbf{2'_a}$, can be reached only via the less stable $\mathbf{3'_a}$ and then intermediate $\mathbf{TS4'_a}$, but the overall barrier (measured from $\mathbf{3'_b}$) is the same in both cases. The data suggest, therefore, that there is little difference, thermodynamically or kinetically, between the pathways that lead to the major and minor isomers.

In conclusion, the aromatic species **1** reacts with H_2 in the absence of a catalyst under relatively mild conditions, cleanly forming the bicyclic species **2a/2b**. The para-H_2 experiments and computational data are consistent with a direct, reversible reaction with H_2 across the 1,4 axis leading to an intermediate 1,3,5-triphosphacyclohexa-1,4-diene analogue. This result demonstrates that access to a boat-shaped conformation with an electrophilic phosphorus center and a nucleophilic carbon center allows for the polar addition of H_2. Subsequent thermally driven hydrogen atom transfer and concurrent P–P bond formation leads to the observed products. This unexpected observation of dihydrogen activation by an aromatic heterocycle provides a new strategy for the design of metal-free hydrogenation catalysts.

■ EXPERIMENTAL SECTION

General Considerations. All manipulations were performed under an atmosphere of dry, oxygen-free N_2 by means of standard Schlenk or glovebox techniques (MBraun glovebox equipped with a −35 °C freezer). All glassware was oven-dried and cooled under vacuum before use. Bromobenzene (D_5) was purchased from Cambridge Isotopes Laboratories, Inc., and was degassed and stored over 4 Å molecular sieves prior to use. NMR spectra were obtained on a Bruker Avance 400 MHz spectrometer or an Agilent DD2 600 MHz spectrometer and spectra were referenced to residual solvent of C_6D_5Br (^{1}H = 7.28 ppm for meta proton; ^{13}C = 122.4 ppm for ipso carbon). Chemical shifts (δ) listed are in ppm and absolute values of the coupling constants are in Hz. Mass spectrometry was performed in house.

X-ray Data Collection, Reduction, Solution, and Refinement. A single crystal of **2a** was coated in paratone-N oil and mounted. The data were collected using the SMART software package on a Siemens SMART System CCD diffractometer using a graphite monochromator with MoKα radiation (λ = 0.71073 Å). Data reduction was performed using the SAINT software package and an absorption correction was applied using SADABS. The structures were solved by direct methods using XS and refined by full-matrix least-squares on F2 using XL as implemented in the SHELXTL suite of programs. All non-hydrogen atoms were refined anisotropically. Carbon-bound hydrogen atoms were placed in calculated positions using an appropriate riding model and coupled isotropic temperature factors.

Synthesis of 1. 2,4,6-Tri-tert-butyl-1,3,5-triphosphabenzene was prepared by a variation on the literature method.[49] To a stirred solution of $Cl_3V=NtBu$[58,59] (0.10 g, 0.44 mmol) in toluene (2 mL) at −30 °C was added tBuCP (0.18 g, 1.76 mmol). The solvent was immediately evaporated under reduced pressure, and the residue was dissolved in n-hexane and purified by flash chromatography on silica gel. Removal of the solvent gave ca. 0.10 g (30%) of yellow crystalline 2,4,6-tri-tert-butyl-1,3,5-triphosphabenzene.

Synthesis of 2. In a 1 dr vial, 15.0 mg (0.05 mmol, 1 equiv) of **1** was weighed and dissolved in C_6D_5Br (0.4 mL), resulting in a bright yellow solution. The solution was transferred to a J-Young tube and sealed. The vessel was degassed three times through freeze–pump–thaw cycles and filled with H_2 (4 atm) at −196 °C. The J-Young tube was then heated to 110 °C in an oil bath, and over 5 h the solution became faint yellow. The C_6D_5Br was removed slowly under reduced pressure yielding diffraction-quality crystals (13 mg). NMR data shows isomers A and B in a 4:1 ratio. Isomers A[3] and B[4] have been previously reported in the literature. The recorded ^{31}P NMR data are in agreement with literature reports; however, the ^{1}H NMR data do not fully correlate with literature values. For both isomers, C3 H can be found in the $C(CH_3)$ chemical shift range (see D_2 experiment and spectrum). ^{1}H NMR (400 MHz, C_6D_5Br, 298 K): δ 2.98 (dd, $^2J_{P-H}$ = 3.9, 1.7 Hz, 1H, A C2 H), 2.59 (t, $^2J_{P-H}$ = 8.2 Hz, 1H, B C2 H), 1.49 (d, $^4J_{P-H}$ = 1.6 Hz, 9H, A C1 tBu), 1.46 (d, $^4J_{P-H}$ = 2 Hz, 9H, B C1 tBu), 1.28 (s, 9H, B C2 tBu), 1.13 (s, 9H, A C2 tBu), 0.93 (s, 9H, B C3 tBu), 0.92 (s, 9H, A C3 tBu). ^{31}P NMR (162 MHz, C_6D_5Br, 298 K): δ 310.2 (dd, $^2J_{P-P}$ = 36.4, 13.1 Hz, A P1), 287.5 (d, $^2J_{P-P}$ = 30.0 Hz, B P1), −117.8 (dd, $^1J_{P-P}$ = 166.2 Hz, $^2J_{P-P}$ = 36.4 Hz, A P2), −128.8 (ddd, $^1J_{P-P}$ = 166.2 Hz, $^2J_{P-P}$ = 13 Hz, $^2J_{P-H}$ = 3.2 Hz, A P3), −135.4 (dd, $^1J_{P-P}$ = 167.0 Hz, $^2J_{P-P}$ = 29.4 Hz, B P2), −171.9 (d, $^1J_{P-P}$ = 167.1 Hz, B P3). HRMS (DART) Calcd for $[C_{15}H_{30}P_3]^+$ ([M + H]$^+$) 303.1560, found 303.1562.

para-Hydrogen Derived Measurements. Hyperpolarized NMR measurements were made on either a Bruker Avance III series 400 MHz NMR spectrometer (^{1}H at 400.13 MHz, ^{13}C at 100 MHz) or a 500 MHz Avance HD system ((^{1}H at 500.13 MHz, ^{13}C at 125 MHz). NMR samples were made up in a Young's tap equipped 5 mm NMR tube and C_6D_5Br (sigma) was used as the solvent. para-Hydrogen was prepared by cooling hydrogen gas over Fe_2O_3 at 30 K. The NMR sample was warmed progressively from 298 K. Upon reaching 375 K, weak PHIP was observed in the ^{1}H NMR signals of **3** at ca. 6.4 (J_{PH} = 228 (d), 6.5 (tr) Hz and J_{HH} = 2 Hz) and 1.8 (J_{PH} = 9.5 (tr), 5.0 (d) Hz and J_{HH} = 2 Hz) ppm. HMQC measurements revealed coupling to two ^{31}P signals at 273.2 and −30.6 ppm. A common ^{31}P splitting of 6.5 Hz is evident in the spectra.

■ ASSOCIATED CONTENT

ⓢ Supporting Information

Full metrical parameters for the solid-state structure of compound **2a** are available free of charge from the Cambridge

13456

dx.doi.org/10.1021/ja5077525 | J. Am. Chem. Soc. 2014, 136, 13453–13457

Crystallographic Data Centre under reference CCDC-1014778. Experimental and crystallographic data are available free of charge via the Internet at http://pubs.acs.org.

■ AUTHOR INFORMATION

Corresponding Author
dstephan@chem.utoronto.ca

Notes
The authors declare no competing financial interest.

■ REFERENCES

(1) Kubas, G. J. *Metal Dihydrogen and σ-Bond Complexes*; Kluwer: New York, 2001.
(2) Heinekey, D. M.; Lledos, A.; Lluch, J. M. *Chem. Soc. Rev.* **2004**, *33*, 175.
(3) McGrady, G. S.; Guilera, G. *Chem. Soc. Rev.* **2003**, *32*, 383.
(4) Jessop, P. G.; Morris, R. H. *Coord. Chem. Rev.* **1992**, *121*, 155.
(5) Burdett, J. K.; Eisenstein, O.; Jackson, S. A. In *Transition Metal Hydrides*; Dedieu, A., Ed.; VCH: New York, 1992; p 149.
(6) Crabtree, R. H. *Acc. Chem. Res.* **1990**, *23*, 95.
(7) Kubas, G. J. *Acc. Chem. Res.* **1988**, *21*, 120.
(8) Ogata, H.; Lubitza, W.; Higuchi, Y. *Dalton Trans.* **2009**, 7577.
(9) Chenevier, P.; Mugherli, L.; Darbe, S.; Darchy, L.; DiManno, S.; Tran, P. D.; Valentino, F.; Iannello, M.; Volbeda, A.; Cavazza, C.; Artero, V. *C. R. Chim.* **2013**, *16*, 491.
(10) Dey, S.; Das, P. K.; Dey, A. *Coord. Chem. Rev.* **2013**, *257*, 42.
(11) Siegbahn, P. E. M. *Adv. Inorg. Chem.* **2004**, *56*, 101.
(12) Sabatier, P. *Ind. Eng. Chem.* **1926**, *18*, 1005.
(13) Calvin, M. *J. Am. Chem. Soc.* **1939**, *61*, 2330.
(14) Coffey, R. S. *Chem. Commun.* **1967**, 923.
(15) Young, J. F.; Osborn, J. A.; Jardine, H.; Wilkinson, G. *Chem. Commun.* **1965**, 131.
(16) Hallman, P. S.; Evans, D.; Osborn, J. A.; Wilkinson, G. *Chem. Commun.* **1967**, 305.
(17) Evans, D.; Osborn, J. A.; Jardine, F. H.; Wilkinson, G. *Nature* **1965**, *208*, 1203.
(18) Schrock, R. R.; Osborn, J. A. *J. Am. Chem. Soc.* **1976**, *98*, 2143.
(19) Schrock, R. R.; Osborn, J. A. *J. Am. Chem. Soc.* **1976**, *98*, 4450.
(20) Schrock, R. R.; Osborn, J. A. *J. Am. Chem. Soc.* **1976**, *98*, 2134.
(21) Knowles, W. S. *Angew. Chem., Int. Ed.* **2002**, *41*, 1998.
(22) Noyori, R. *Angew. Chem., Int. Ed.* **2002**, *41*, 2008.
(23) Zuo, W. W.; Lough, A. J.; Li, Y. F.; Morris, R. H. *Science* **2013**, *342*, 1080.
(24) Bullock, R. M. *Science* **2013**, *342*, 1054.
(25) Jagadeesh, R. V.; Surkus, A. E.; Junge, H.; Pohl, M. M.; Radnik, J.; Rabeah, J.; Huan, H. M.; Schunemann, V.; Bruckner, A.; Beller, M. *Science* **2013**, *342*, 1073.
(26) Berkessel, A.; Schubert, T. J. S.; Mueller, T. N. *J. Am. Chem. Soc.* **2002**, *124*, 8693.
(27) Spielmann, J.; Buch, F.; Harder, S. *Angew. Chem., Int. Ed.* **2008**, *47*, 9434.
(28) Xiao, Z. L.; Hauge, R. H.; Margrave, J. L. *Inorg. Chem.* **1993**, *32*, 642.
(29) Himmel, H. J.; Vollet, J. *Organometallics* **2002**, *21*, 11626.
(30) Himmel, H. J. *Dalton Trans.* **2003**, 3639.
(31) Kulkarni, S. A. *J. Phys. Chem. A* **1998**, *102*, 7704.
(32) Kulkarni, S. A.; Srivastava, A. K. *J. Phys. Chem. A* **1999**, *103*, 2836.

(33) Spikes, G. H.; Fettinger, J. C.; Power, P. P. *J. Am. Chem. Soc.* **2005**, *127*, 12232.
(34) Stephan, D. W.; Erker, G. *Top. Curr. Chem.* **2013**, *332*, 85.
(35) Stephan, D. W. *Org. Biomol. Chem.* **2012**, *10*, 5740.
(36) Paradies, J. *Angew. Chem., Int. Ed.* **2014**, *53*, 3552.
(37) Welch, G. C.; Juan, R. R. S.; Masuda, J. D.; Stephan, D. W. *Science* **2006**, *314*, 1124.
(38) Power, P. *Nature* **2010**, *463*, 171.
(39) Frey, G. D.; Lavallo, V.; Donnadieu, B.; Schoeller, W. W.; Bertrand, G. *Science* **2007**, *316*, 439.
(40) Fan, C.; Mercier, L. G.; Piers, W. E.; Tuononen, H. M.; Parvez, M. *J. Am. Chem. Soc.* **2010**, *132*, 9604.
(41) Hadlington, T. J.; Hermann, M.; Li, J. Y.; Frenking, G.; Jones, C. *Angew. Chem., Int. Ed.* **2013**, *52*, 10199.
(42) Clayden, J.; Greeves, N.; Warren, S.; Wothers, P. *Organic Chemistry*; Oxford University Press: New York, 2001.
(43) Dyson, P. J. *Dalton Trans.* **2003**, 2964.
(44) Glorius, F. *Org. Biomol. Chem.* **2005**, *3*, 4171.
(45) Wang, D.-S.; Chen, Q.-A.; Lu, S.-M.; Zhou, Y.-G. *Chem. Rev.* **2012**, *112*, 2557.
(46) Chen, Q.-A.; Ye, Z.-S.; Duan, Y.; Zhou, Y.-G. *Chem. Soc. Rev.* **2013**, *42*, 497.
(47) Borowski, A. F.; Sabo-Etienne, S.; Donnadieu, B.; Chaudret, B. *Organometallics* **2003**, *22*, 1630.
(48) Mahdi, T.; Heiden, Z. M.; Grimme, S.; Stephan, D. W. *J. Am. Chem. Soc.* **2012**, *134*, 4088.
(49) Tabellion, F.; Nachbauer, A.; Leininger, S.; Peters, C.; Preuss, F.; Regitz, M. *Angew. Chem., Int. Ed.* **1998**, *37*, 1233.
(50) Gleiter, R.; Lange, H.; Binger, P.; Stannek, J.; Krüger, C.; Bruckmann, J.; Zenneck, U.; Kummer, S. *Eur. J. Inorg. Chem.* **1998**, 1619.
(51) Nyulaszi, L. *Chem. Rev.* **2001**, *101*, 1229.
(52) Townsend, N. S.; Green, M.; Russell, C. A. *Organometallics* **2012**, *31*, 2543.
(53) Hofmann, M.; Schleyer, P.; Regitz, M. *Eur. J. Org. Chem.* **1999**, 3291.
(54) Binger, P.; Stutzmann, S.; Stannek, J.; Günther, K.; Phillips, P.; Mynott, R.; Bruckmann, J.; Krüger, C. *Eur. J. Inorg. Chem.* **1999**, 763.
(55) Jones, C.; Waugh, M. *Dalton Trans.* **2004**, 1971.
(56) Russell, C. A.; Townsend, N. S. In *Phosphorus(III) Ligands in Homogeneous Catalysis: Design and Synthesis*; Kamer, P. C. J., Leeuwen, P. W. N. M. v., Eds.; John Wiley & Sons Ltd.: New York, 2012; p 343.
(57) Hills, A.; Hughes, D.; Leigh, G. J.; Prieto-Alcon, R. *J. Chem. Soc., Dalton Trans.* **1993**, 3609.
(58) Preuss, F.; Towae, W. *Z. Naturforsch. B* **1981**, *36*, 1130.
(59) Fuchslocher, E.; Towae, W.; Leber, E. *Z. Naturforsch. B* **1989**, *44*, 271.
(60) Bowers, C. R.; Weitekamp, D. P. *J. Am. Chem. Soc.* **1987**, *109*, 5541.
(61) Duckett, S. B.; Mewis, R. E. *Acc. Chem. Res.* **2012**, *45*, 1247.
(62) Zhivonitko, V. V.; Telkki, V. V.; Chernichenko, K.; Repo, T.; Leskela, M.; Sumerin, V.; Koptyug, I. V. *J. Am. Chem. Soc.* **2014**, *136*, 598.
(63) Aguilar, J. A.; Adams, R. W.; Duckett, S. B.; Green, G. G. R.; Kandiah, R. *J. Magn. Reson.* **2011**, *208*, 49.
(64) Koch, W.; Holthausen, M. *A Chemist's Guide to Density Functional Theory*; Wiley-VCH: Weinheim, 2000.
(65) Grimme, S. *J. Comput. Chem.* **2006**, *27*, 1787.
(66) Grimme, S.; Antony, J.; Ehrlich, S.; Krieg, H. *J. Chem. Phys.* **2010**, *132*, 154104.
(67) Grimme, S.; Ehrlich, S.; Goerigk, L. *J. Comput. Chem.* **2011**, *32*, 1456.
(68) Møller, C.; Plesset, M. S. *Phys. Rev. A* **1934**, *46*, 618.
(69) Hadlington, T. J.; Hermann, M.; Li, J.; Frenking, G.; Jones, C. *Angew. Chem., Int. Ed.* **2013**, *52*, 10199.
(70) Zhong, G.; Chan, B.; Radom, L. *J. Am. Chem. Soc.* **2007**, *129*, 924.